Competitive Binding of Natural Amphiphiles with Graphene Derivatives

Slaven Radic, Nicholas K. Geitner, Ramakrishna Podila, Pu Chun Ke and Feng Ding

Department of Physics and Astronomy, COMSET, Clemson University, Clemson, South Carolina 29634, United States
E-mail: fding@clemson.edu; pcke11@clemson.edu

ABSTRACT

Understanding the transformation of graphene derivatives by natural amphiphiles is essential for elucidating the biological and environmental implications of this emerging class of engineered nanomaterials. Using rapid discrete-molecular-dynamics simulations, we examined the binding of graphene and graphene oxide with peptides, fatty acids, and cellulose, and complemented our simulations by experimental studies of UV-Vis spectrophotometry. Specifically, we established a connection between the differential binding and the conformational flexibility, molecular geometry, and hydrocarbon content of the amphiphiles. This study provides a mechanistic basis for addressing the transformation, evolution, transport, biocompatibility, and toxicity of graphene derivatives in living systems and the natural environment.

1 INTRODUCTION

Due to their unique physical properties [1], graphene and graphene derivatives have emerged as ideal materials for constructing novel nano- and quantum devices. The potential applications of graphene derivatives range from electronic circuits and energy storage to biomedical nanodevices for imaging, sensing, and diagnosis [2-6]. It has become increasingly crucial to delineate the transformation, evolution, transport, and biocompatibility of graphene derivatives in the aqueous phase, ranging from biological to environmental systems [7]. Once discharged into the environment or introduced to biological systems, graphene derivatives may interact with natural organic matter, biomolecules, and other ionic and molecular complexes through self assembly and chemical reactions. Most of these natural and bio-materials are amphiphilic in nature, and are usually comprised of carbohydrates, peptides, and fatty acids. Since natural amphiphiles may bind with graphene derivatives to render a biocorona [8, 9], it is conceivable that the fate of graphene derivatives in biological systems and the environment is determined by the entity of the biocorona rather than the nanomaterial substrates alone. Furthermore, differences in the concentration and affinity of natural amphiphiles may lead to their competitive binding for graphene derivatives, similar to the Vroman effect that is exhibited by serum proteins adsorbed onto solid surfaces [10].

A systematic study of the binding of graphene derivatives with a collection of representative natural amphiphiles is essential for elucidating the transformation and dynamics of graphene derivatives in complex biological and environmental media. Specifically for simulations, we adopted cellulose dimers, tri-alanine peptides, and palmitic acids as model amphiphiles to represent the sugar, peptide, and fatty acid moieties present in algal exudates used in our experiments, respectively. In addition to being prevalent in aquatic environments, these molecular species are also ubiquitous across the biosphere of living organisms. We performed discrete molecular dynamics (DMD) simulations, a rapid dynamic sampling algorithm [11] to characterize the binding between the graphene derivatives and the natural amphiphiles. In our simulations, graphene nanosheet was presented as a two-dimensional honeycomb, where its aromatic carbon atoms featured van der Waals and hydrophobic interactions. In contrast, graphene oxide was modeled by introducing defects, epoxidations, hydroxylations, and carboxylations to its graphene backbone.

2 RESULTS

2.1. Differential Binding of Nanosheets with Single Amphiphiles: Temperature Varying DMD Simulations.

We first characterized the dynamics of single-molecular binding between the nanosheets of graphene derivatives and the amphiphiles. We

performed DMD simulations at different temperatures and monitored the binding along the simulation trajectories. In the case of graphene oxide and cellulose binding, we observed three different regimes (Fig. 1).

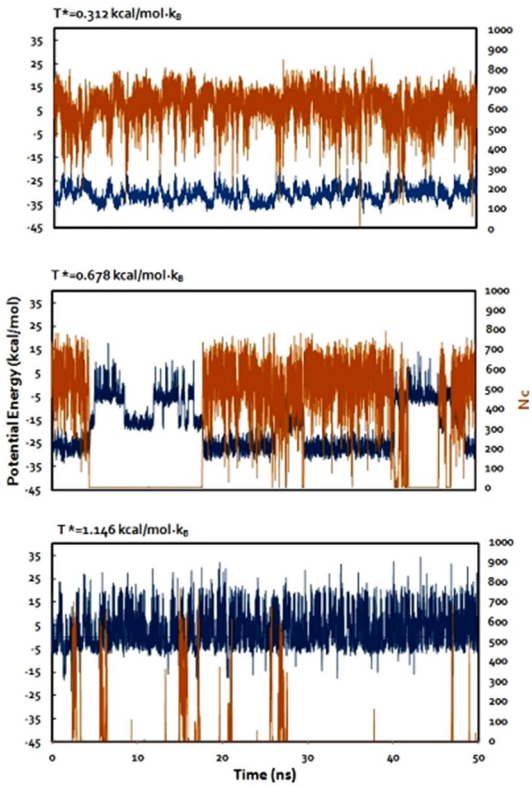

Figure 1. Binding simulation trajectories at different temperatures. Both potential energy (E, blue, left vertical axis) and number of atomic contacts (N_c, orange, right vertical axis) are shown for DMD simulations of cellulose-graphene oxide binding. Simulations at three different temperatures are shown: T*=0.312 (a), 0.678 (b), and 1.146 (c), where the temperature unit is kcal/mol·k_B.

At low temperatures (Fig. 1a), the molecular system had low potential energies and the cellulose stayed bound to the nanosheet with a high number of atomic contacts (N_c) occurring between the two species. At high temperatures (Fig. 1c), the cellulose molecule dissociated from the nanosheet with higher potential energies and a low N_c value. The two species only occasionally formed contacts due to thermal fluctuations. Between these two extreme regimes, there existed a mid-point temperature, T_m, where the cellulose had approximately an equal probability of being bound and unbound to graphene oxide (Fig. 1b). Interestingly, in the unbound state, the systems featured an intermediate energy state, which belonged to the excitation of a high-energy normal mode due to harmonic constraint applied to confine the nanosheet. Therefore, the inter-molecular contact, N_c, rather than the potential energy, was a more appropriate parameter to monitor the binding. At T_m, the potential energies and inter-molecular N_c values displayed large and anti-correlated fluctuations, clearly resulting from the interplay of enthalpy and entropy. Here the contributions of entropy include freedoms in both translation and configuration. The values of T_m were used to quantify the binding affinities between the different amphiphiles and the nanosheets.

Accurate estimation of T_m requires sufficient sampling of the conformational space. We therefore applied replica exchange DMD simulations [12] to enhance the sampling, where multiple simulations were running in parallel at different temperatures and the replica temperatures were subject to exchange periodically according to the Metropolis criteria [13] Based on the replica exchange simulations, we computed the thermodynamic parameters using the weighted histogram method [14]. We computed the average N_c as a function of temperature (Fig. 1a). For comparison between different molecular systems, we normalized the average N_c by its maximum value at low temperature to obtain the Q-value, which quantified the fraction of inter-molecular contacts. The amphiphiles showed a lower T_m when bound to graphene oxide than graphene, indicating a weaker binding associated with graphene oxide due to its various surface modifications that compromised inter-molecular hydrophobic interaction while encouraged electrostatic repulsion. Palmitic acid displayed the strongest binding while tri-alanine showed the weakest (Fig. 2).

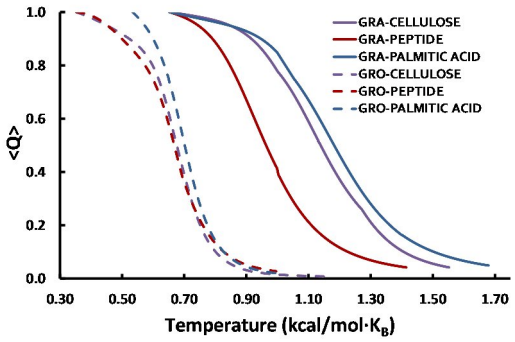

Figure 2. The temperature dependence of <Q> values illustrates the melting.

The strong binding of palmitic acid to the nanosheets correlated with its longer molecular chain that consisted of a higher number of hydrocarbons and hence a greater degree of chain flexibility. In addition, the higher melting temperature for cellulose on graphene, compared to that for peptide, can be attributed to stacking. In contrast to the ring-like structure of the cellulose, the peptide backbone of tri-alanine was unable to form many contacts with the nanosheet. This is in agreement with the molecular dynamics study by Katoch *et al.,* in which a lower binding affinity was observed when tryptophan residues were replaced by alanine. In the case of graphene oxide, the melting curves for cellulose and peptide were closer to each other (Fig. 2), suggesting that stacking was compromised by the functional groups of the nanosheet to shield its aromatic structure.

2.2. Differential Binding of Nanosheets with Single Amphiphiles: Experimental results

To complement the simulations, algal exudates were acquired from freshly cultured *Chlorella* sp. following a protocol developed in our lab [15]. The algal exudates were used to mimic the natural amphiphiles of cellulose, peptides, and fatty acids in the simulations. To examine the binding kinetics of graphene and graphene oxide with algal exudates, we incubated the nanosheets with exudates in water and observed their precipitation at different temperatures. The absorbance peak of the algal exudates at 205 nm was monitored over time for both graphene and graphene oxide (Figs. 3a, b).

The normalized absorbance value corresponded to the total fraction of exudates and graphene (graphene oxide) still present in solution at a given time. This process was performed with fresh suspensions at both 30ºC and 35ºC. Control experiment of graphene and graphene oxide in the absence of algal exudates was performed at both temperatures, and we did not identify significant temperature dependence of the control precipitation over the temperature range examined. For both graphene and graphene oxide, algal exudates slowed the rate of precipitation at both temperatures. This general behavior is indicative of exudates binding with graphene and graphene oxide to render both types of nanosheets more water-soluble. The binding with algal exudates should also discourage π-stacking of the nanosheets, further slowing their rate of precipitation.

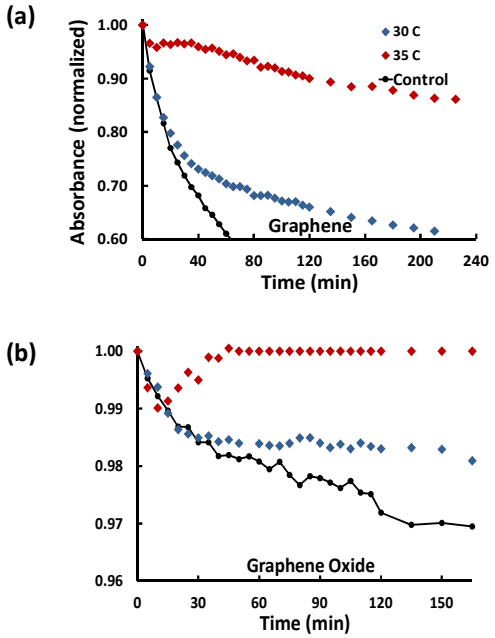

Figure 3. UV-Vis absorbance spectra of algal exudates mixed with graphene (a) and graphene oxide (b) measured at 30°C (blue) and 35°C (maroon). Control kinetics performed in the absence of exudates at 30ºC (with no significant difference seen at 35ºC) at concentrations equal to test samples.

2.3. Differential Binding of Nanosheets with Multiple Amphiphile Species: DMD Simulation

To model the binding of graphene derivatives with a collection of natural amphiphiles in biological and environmental media, we performed a constant-temperature DMD simulation of a graphene oxide nanosheet mixed with the three amphiphilie species simultaneously. We used the relative ratios of glucose to peptide to palmitic acid as found in algal exudates, 7:3:1, and accordingly we included 14 cellulose, 6 peptide, and 2 palmitic acid molecules. The amphiphilic molecules were initially positioned away from the nanosheet (Fig. 4a). We chose a simulation temperature $T \approx T_m$ of tri-alanine binding. This temperature allowed rapid equilibration while all molecules were able to bind to the graphene oxide nanosheet. We then monitored the number density of molecules bound to the nanosheet along the simulation trajectory (Fig. 4b). Due to their high

concentrations, peptides and celluloses rapidly covered the nanosheet to form a nanosheet-amphiphile biocorona (0-8 ns; Figs. 4a, b), which hindered the binding of palmitic acids. However, due to their relatively weak binding affinity, the peptides and celluloses on the nanosheet underwent rapid exchange with the molecules in solution to assume a "soft" biocorona. Despite having the lowest concentration in the simulation, palmitic acids occasionally interacted with the dynamic biocorona under diffusion. Once the nanosheet was available, a palmitic acid bound to its surface and remained bound during the course of the simulation (e.g., > 25 ns; Fig. 4b). As a result, the biocorona became "hardened" as evidenced by the smaller fluctuations of the number of nanosheet-bound molecules after both palmitic acids were attached to the surface (t > 35 ns; Fig. 4b). In the case of higher stoichiometric ratios of amphiphiles to the nanosheet, we expect a complete coverage of the nanosheet by strong binders like the palmitic acids to render a "hard" biocorona. Our results illustrate the general applicability of the Vroman effect for describing the binding kinetics of biomolecular species competing for graphene derivatives.

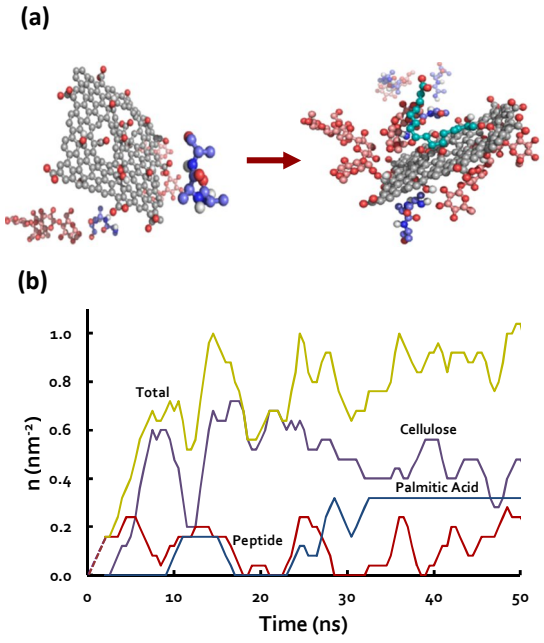

Figure 4. Vroman-like competitive binding of amphiphile mixture with graphene oxide. (a) The DMD simulation snapshots of the binding between graphene oxide and amphiphile mixture: t=0 ns and 50 ns. (b) The number density of molecules, *n*, bound to the nanosheet is shown along the simulation trajectory.

REFERENCES

[1] K. S. Novoselov, *et al.* Electric Field Effect in Atomically Thin Carbon Films. *Science* 306, 666, 2004.

[2] Q. He, *et al.* Graphene-based Electronic Sensors. *Chem. Sci.* 3, 1764, 2012.

[3] W. Yang, *et al.* Carbon Nanomaterials in Biosensors: Should You Use Nanotubes or Graphene? *Angew. Chem.-Int. Edit.* 49, 2114, 2010.

[4] J.-D. Qiu, J. Huang and R.-P. Liang, Nanocomposite Film Based on Graphene Oxide for High Performance Flexible Glucose Biosensor. *Sens. Actuator B-Chem.* 160, 287, 2011.

[5] E. Morales-Narvaez and A. Merkoci, Graphene Oxide as an Optical Biosensing Platform. *Adv. Mater.* 24, 3298, 2012.

[6] K. Yang, L. Feng, X. Shi and Z. Liu, Nano-Graphene in Biomedicine: Theranostic Applications. *Chem. Soc. Rev.* 42, 530, 2013.

[7] K. Wang, *et al.* Biocompatibility of Graphene Oxide. *Nanoscale Research Letters* 6, 8, 2010.

[8] T. Cedervall, *et al.* Understanding the Nanoparticle-Protein Corona Using Methods to Quantify Exchange Rates and Affinities of Proteins for Nanoparticles. *Proc. Natl. Acad. Sci. U. S. A.* 104, 2050, 2007.

[9] P. C. Ke, Fiddling the String of Carbon Nanotubes with Amphiphiles. *Phys. Chem. Chem. Phys.* 9, 439, 2007.

[10] V. Hlady and J. Buijs, Protein Adsorption on Solid Surfaces. *Curr. Opin. Biotechnol.* **7**, 72, 1996.

[11] D. C. Rapaport, *The Art of Molecular Dynamics Simulation*. (Cambridge University Press, 2004).

[12] F. Ding, D. Tsao, H. Nie and N. V. Dokholyan, Ab Initio Folding of Proteins with All-atom Discrete Molecular Dynamics. *Structure* 16, 1010, 2008.

[13] N. Metropolis and S. Ulam, The Monte Carlo Method. *J. Am. Stat. Assoc.* 44, 335, 1949.

[14] J. D. Chodera, W. C. Swope, J. W. Pitera, C. Seok and K. A. Dill, Use of the Weighted Histogram Analysis Method for the Analysis of Simulated and Parallel Tempering Simulations. *J. Chem. Theory Comput.* 3, 26, 2007.

[15] P. Chen, B. A. Powell, M. Mortimer and P. C. Ke, Adaptive Interactions between Zinc Oxide Nanoparticles and Chlorella sp. *Environ. Sci. Technol.* 46, 12178, 2012.